MHC ligand generation in T cell-mediated immunity and MHC multimer technologies for T cell detection

Bakker, A.H.

Chapter 2

Analysis of protease activity in live antigen–presenting cells shows regulation of the phagosomal proteolytic contents during dendritic cell activation

Ana–Maria Lennon–Duménil*, Arnold H. Bakker*, René Maehr, Edda Fiebiger, Herman S. Overkleeft, Mario Rosemblatt, Hidde L. Ploegh, and Cécile Lagaudrière–Gesbert

J Exp Med. 2002 Aug 19;196(4):529–40

(* these authors contributed equally to this work)

Analysis of Protease Activity in Live Antigen-presenting Cells Shows Regulation of the Phagosomal Proteolytic Contents During Dendritic Cell Activation

Ana-Maria Lennon-Duménil,[1] Arnold H. Bakker,[1] René Maehr,[1] Edda Fiebiger,[1] Herman S. Overkleeft,[1] Mario Rosemblatt,[2] Hidde L. Ploegh,[1] and Cécile Lagaudrière-Gesbert[1]

[1]*Department of Pathology, Harvard Medical School, Boston, MA 02115*
[2]*Departamento de Biologia, Facultad de Ciencias, Universidad de Chile, 6842301 Santiago, Chile*

Abstract

Here, we describe a new approach designed to monitor the proteolytic activity of maturing phagosomes in live antigen-presenting cells. We find that an ingested particle sequentially encounters distinct protease activities during phagosomal maturation. Incorporation of active proteases into the phagosome of the macrophage cell line J774 indicates that phagosome maturation involves progressive fusion with early and late endocytic compartments. In contrast, phagosome biogenesis in bone marrow–derived dendritic cells (DCs) and macrophages preferentially involves endocytic compartments enriched in cathepsin S. Kinetics of phagosomal maturation is faster in macrophages than in DCs. Furthermore, the delivery of active proteases to the phagosome is significantly reduced after the activation of DCs with lipopolysaccharide. This observation is in agreement with the notion that DCs prevent the premature destruction of antigenic determinants to optimize T cell activation. Phagosomal maturation is therefore a tightly regulated process that varies according to the type and differentiation stage of the phagocyte.

Key words: antigen processing • cathepsin • active site–directed probe • phagocytosis • phagosomal maturation

Introduction

MHC class II molecules expressed on the surface of APCs present antigenic peptides to $CD4^+$ T lymphocytes. These peptides are produced mainly from antigens that have been internalized and processed in the endocytic pathway of APCs, where they meet class II molecules en route to the cell surface (1, 2). APCs acquire antigens via endocytosis, either nonspecifically or through receptors expressed on their surface (1, 3). The main function of antigen receptors is to target and concentrate antigen in intracellular compartments competent for processing and for interaction of the resulting digestion products with class II molecules (1, 3).

Endocytic proteases play a key role in two different steps of MHC class II–restricted antigen presentation: invariant chain cleavage and antigen degradation. Indeed, invariant chain, which directs class II molecules to the endocytic pathway and protects them from premature peptide binding, must be proteolyzed in endosomal compartments to allow its replacement with peptide antigen. The cysteine proteases cathepsin (Cat)*S and CatL are implicated in this process (4–6). Antigen processing involves many hydrolase activities present along the endocytic pathway of APCs (6–8). Among these enzymes are the γ-interferon–inducible lysosomal thiol reductase (9, 10), and several cysteine proteases including CatB, CatS, CatL, and asparaginyl endopeptidase (4–8). Limited proteolysis rather than total breakdown of antigens is the rule, because MHC class II molecules present peptides of 9 to 16 residues to $CD4^+$ T cells (2). Therefore, a balanced proteolytic environment is required to ensure adequate processing while preventing complete destruction. The molecular mechanisms that control trafficking and exposure of antigens to endocytic proteases are poorly understood.

Phagocytosis is probably a dominant mode of antigen uptake in vivo for professional APCs such as dendritic cells (DCs) and macrophages (11). Phagosomes formed by APCs after uptake of latex beads have been shown to be fully

A.M. Lennon-Duménil and A.H. Bakker contributed equally to this work.

Address correspondence to Hidde L. Ploegh, Department of Pathology, 200 Longwood Avenue, Building 2, Room 137, Boston, MA 02115. Phone: 617-432-4777; Fax: 617-432-4775; E-mail: ploegh@hms.harvard.edu

*Abbreviations used in this paper: Cat, cathepsin; ConB, concanamycin B; DC, dendritic cell; MACS, magnetic-activated cell sorting.

equipped for antigen processing and peptide loading (12). How do phagosomes acquire the proteolytic activities necessary to degrade antigens? The macrophage cell line J774 is a well-characterized model for analysis of phagosome biogenesis (13, 14). In J774 cells, newly formed phagosomes undergo progressive maturation by fusing sequentially with the early endosomal, late endosomal, and lysosomal compartments (13). A proteomic analysis of latex bead–containing phagosomes in J774 cells identified >140 proteins detected at different stages of phagosomal biogenesis (15). In particular, endocytic proteases from the Cat family are gradually incorporated into the phagosome during its maturation, suggesting that these proteases are found all along the endocytic edge, including early endosomes (15). However, whether these enzymes are active in these nonacidic compartments remains to be addressed.

Endocytic proteases are synthesized as inactive zymogens, including a propeptide that is located at the NH_2 terminus of the protein and occupies their active site, thus preventing premature enzymatic activity (6–8). Once in endosomal compartments, the drop in the pH promotes the removal of the propeptide and conversion to the active, mature protease (6–8). The molecular weight of endosomal proteases can therefore be indicative of their state of activation. However, the activity of these enzymes is also set by the milieu in which they function (pH conditions and the presence of small competitive inhibitors; references 6, 7, and 16). The activity of cysteine proteases can be visualized ex vivo in crude cell extracts using fluorescent substrates or active site–directed probes (17). The latter correspond to electrophilic substrate analogs that are subject to nucleophilic attack by the cysteine residue in the protease active site. This reaction modifies the enzyme so that it is now covalently and irreversibly attached to the probe. Because the covalent modification by these probes is mechanism-based, the intensity of labeling is proportional to protease activity (17, 18).

Here, we describe an in vivo approach to monitor the proteolytic environment encountered by phagocytosed particles upon internalization into the APC. By loading latex beads with an active site–directed probe, we analyzed the activity of the proteases incorporated into the phagosome during biogenesis. This method was first validated using the monocytic cell line J774, and then applied to peritoneal macrophages, bone marrow–derived macrophages, and DCs. Our results indicate that the proteolytic contents of the phagosome depend on both the differentiation stage of the APC and the extracellular stimuli. This implies that the proteolytic environment to which particulate antigens are exposed in the APC is under tight regulation.

Materials and Methods

Mice. C57BL/6 mice were purchased from The Jackson Laboratory. CatB, CatS, and CatL knockout mice have been previously described (19).

Cells and Culture Conditions. J774, a mouse promonocytic cell line, and RAW264.7, a mouse monocyte/macrophage cell line, were obtained from the American Type Culture Collection and were cultured in RPMI 1640 supplemented with 2 mM glutamine, 10% FCS, and antibiotics.

For the preparation of bone marrow–derived APCs, bone marrow was obtained from 2–4-mo-old mice and APCs were prepared as previously described (20), by culturing in RPMI 1640 with 10% FCS supplemented with 10 ng/ml recombinant mouse GM-CSF (PeproTech). Culture medium was changed at days 2 and 4, and cells were harvested at day 5 or 6. Magnetic cell sorting with anti-CD11c antibody–coated beads was used to separate bone marrow–derived DCs from macrophages according to the manufacturer's protocol (magnetic-activated cell sorting [MACS]; Miltenyi Biotec). Single cell suspensions were preincubated with goat serum and Fc Block (BD Biosciences) for 20 min at 4°C before magnetic separation. After sorting, cells were incubated with anti-CD11c or anti–I-A^b antibodies (BD Biosciences) and cytofluorometric analysis was performed on a FACScan™ using CELL Quest™ software (Becton Dickinson). Inflammatory peritoneal macrophages were generated as previously described (21).

Active Site Labeling of Cysteine Proteases in Cell Lysates. JPM-565 and DCG-04 were synthesized and purified as previously described (18, 22). Cell lysates were prepared in lysis buffer (50 mM sodium acetate, pH 5, 5 mM $MgCl_2$, 0.5% NP-40) and protein concentration was measured using the Bi-cinchonic acid protein assay (Pierce Chemical Co.). Lysates (25 μg protein/sample) were incubated with DCG-04 for 60 min at 37°C. After boiling in reducing sample buffer for 10 min, samples were analyzed by 12.5% SDS-PAGE and transferred to a polyvinylidene membrane. After blocking with PBS-10% nonfat milk, the membrane was probed with a 1:1,000 dilution of streptavidin–horseradish peroxidase (Amersham Biosciences) in PBS-0.2% Tween 20 for 60 min followed by five washes with PBS-0.2% Tween 20. Enhanced chemiluminescence was used for visualization. We did not observe any difference in the labeling pattern when including 5 mM dithiothreitol in the lysis buffer (unpublished data).

Immunoprecipitation. Cell lysates (100 μg protein) were incubated with 50 μM DCG-04 in 50 μl lysis buffer, pH 5, for 60 min at 37°C. SDS was added to a final concentration of 1%. Samples were boiled for 5 min and the volume was adjusted to 1.5 ml using pH 7.4 lysis buffer (50 mM Tris-HCl, pH 7.4, 5 mM $MgCl_2$, 0.5% NP-40). Immunoprecipitations were performed as previously described (23) using 5 μl anti-CatL (provided by A. Erikson, University of North Carolina, Chapel Hill, NC; reference 24), 5 μl anti-CatB serum, or 1 ml of the cell culture supernatant from a hybridoma producing an anti-CatS mAb. Samples were analyzed by 12.5% SDS-PAGE and streptavidin blotting.

Purification and Identification of Cysteine Proteases. J774 cell lysates (8–10 mg total protein) were incubated with 5 μM DCG-04 for 60 min at 37°C. As controls, one sample was preincubated with 25 μM JPM-565 for 60 min before the addition of DCG-04, and for another sample the addition of DCG-04 was omitted. Purification of DCG-04–labeled cysteine proteases was performed with streptavidin agarose as previously described (18), except that 0.5% SDS was added and the samples were boiled before purification over the PD-10 column. Samples were run on a 12.5% SDS-PAGE. 1/25 was used for detection by streptavidin blotting. The remainder was Coomassie stained as follows: the gel was fixed in H_2O/25% isopropanol/10% acetic acid for 45 min, stained with 10% acetic acid/0.006% Coomassie brilliant blue G (Sigma-Aldrich) overnight, and destained with 10% acetic acid for 2 h. Polypeptides retrieved on the DCG-04 matrix were excised, digested with trypsin, and analyzed by mass spectrometry using an ion trap liquid chromatography tandem mass spectrome-

try system (performed by Steven Gygi, Harvard Medical School, Boston, MA).

Subcellular Fractionation. J774 cells were grown in 20-cm dishes. For each time point, three dishes (10^7 cells/dish) were used. Cells were pulsed with 2 μm YG fluorescent beads (250 μl/dish; Polysciences) at 37°C, washed three times for 10 min at 4°C with PBS to remove excess beads, and chased at 37°C. Bead-containing compartments were isolated on a sucrose gradient as previously described (13). After centrifugation, both the fluorescent bead–containing compartments and the membranes free of beads were collected, and reducing SDS sample buffer was added. After boiling, proteins were separated by 12.5% SDS-PAGE and streptavidin blotting.

Active Site Labeling of Cysteine Proteases in Live Cells. Cell lines were plated on 12-well plates (0.5×10^6 cells/well) 1 d before the experiment. Streptavidin-coated carboxylated latex beads (1- or 2-μm diameter; Polysciences) were incubated with DCG-04 for 60 min at room temperature. Beads were washed twice with PBS and resuspended in complete culture medium. Plated cells were washed and pulsed at 37°C with 500 μl medium containing DCG-04–coated beads for different times. Cells were then washed three times with medium by agitation to remove excess beads and then incubated in medium for different times at 37°C. Medium was removed and cells were lysed with 100 μl of 2× hot reducing SDS sample buffer, supplemented or not with 100 μM free JPM-565. Lysates were harvested, boiled, and the DNA was sheared with a syringe or sonication. Samples were analyzed by 12.5% SDS-PAGE and streptavidin blotting.

Bone marrow GM-CSF cultures were harvested after 5 or 6 d and pulsed in suspension with DCG-04–coated beads for 5 min at 37°C. In some experiments, 0.1 μg/ml LPS was added to the cells during the pulse. After the pulse, excess beads were removed by centrifuging them four times at 500 *g* for 2 min over an FCS cushion. $CD11c^+$ and $CD11c^-$ cells were separated by MACS. Equal cell numbers (10^6) of both populations were incubated for different times in complete medium at 37°C. Cells were centrifuged in the well for 5 min at 1,000 *g* and lysed with hot 2× SDS reducing sample buffer containing 100 μM JPM-565. The lysates were harvested, boiled, and the DNA was sheared with a syringe or sonication. Half of the sample was analyzed by 12.5% SDS-PAGE and streptavidin blotting. Identical experiments were performed with murine peritoneal macrophages harvested 4 d after thioglycollate medium injection.

Results

We devised a strategy to sample the proteolytic environment encountered by phagocytosed antigens in professional APCs. For this purpose, we used the biotinylated active site–directed probe, DCG-04, coupled to streptavidin-coated latex beads. DCG-04 is a derivative of the peptide epoxide JPM-565 and specifically targets cysteine proteases (Fig. 1 B; reference 18). Probe-coated beads are internalized by APCs through phagocytosis. Bead-containing phagosomes undergo maturation by fusion with the different endocytic compartments of the APC. Once inside the cell, the active site–directed probe senses its proteolytic environment by reacting with active proteases incorporated into the phagosome (Fig. 1 A). This scenario presupposes that probes immobilized via biotin to the latex beads remain available for interaction with proteases via their COOH-terminal epoxide moiety. Because binding of the probe to the protease active site is covalent and irreversible, proteases labeled in vivo can then be visualized after direct lysis of the phagocytes in SDS sample buffer, followed by simple electrophoresis and streptavidin blotting. For a given protease, different labeling intensities correspond directly to differences in activity levels. This approach should therefore allow us to evaluate the activity of individual cysteine proteases delivered to the phagosome of APCs during its maturation.

Cysteine Proteases Recognized by the Active Site–directed Probe DCG-04 in Macrophages. The active site–directed probes JPM-565 and its biotinylated version DCG-04 consist of an epoxide moiety linked to a tyrosine and leucine residue with the biotinylated form containing an additional lysine for the attachment of the biotin moiety (Fig. 1 B; references 17, 18, and 22). In crude cell extracts, JPM-565 is a specific inhibitor of cysteine proteases of the papain family including CatB, CatL, and CatS (17). DCG-04 has a specificity very similar to that of JPM-565 and labels CatB, CatH, CatL, CatZ, and CatC in rat liver cell extracts (18). Neither JPM-565 nor DCG-04 are cell permeable as such.

To establish our in vivo protease labeling assay, we used the J774 monocytic cell line, which has been extensively characterized in terms of phagosomal biogenesis using latex beads (13, 15). To identify the targets of DCG-04 in J774 cells, lysates were prepared at pH 5 and incubated with an increasing amount of the DCG-04, followed by SDS-PAGE and streptavidin blotting (Fig. 1 C). At least seven distinct polypeptides were detected in the 20–40-kD range, where most of the known active cysteine proteases are expected to migrate. To identify these proteases, DCG-04–labeled cell lysates were immunoprecipitated with antibodies directed against CatB, CatL, and CatS. This allowed the identification of three major DCG-04–labeled species as being CatB, CatL, and CatS (Fig. 1 D). The identity of these enzymes was additionally confirmed by comparing the labeling pattern of WT and CatB-, CatS-, or CatL-deficient cells (Fig. 4 B). The polypeptide strongly reactive with DCG-04 and of a mass slightly larger than that of CatB did not react with any of the antibodies tested (Fig. 1 C), including a CatH antiserum (unpublished data). DCG-04–labeled cell lysates were therefore incubated with streptavidin-coated agarose beads on a preparative scale and bound material was resolved by electrophoresis followed by Coomassie staining. The polypeptide of interest was excised, digested with trypsin, and analyzed by microbore and electron spray mass spectrometry, allowing its unambiguous identification as CatZ. The three top bands detected in J774 lysates (Fig. 1, C and D) were not considered in our analysis because they were never detected in in vivo labeling assays (see below).

In conclusion, DCG-04 recognizes CatB, CatS, CatL, and CatZ in crude cell extracts from J774 cells. Proteomic analysis of latex bead–containing phagosomes in the J774 cell line has shown that CatB, CatS, CatL, and CatZ are indeed the most abundant cysteine proteases incorporated into the phagosome during maturation (15), although the activity of these proteases could not directly be assessed by this proteomic approach. Therefore, DCG-04 is a probe

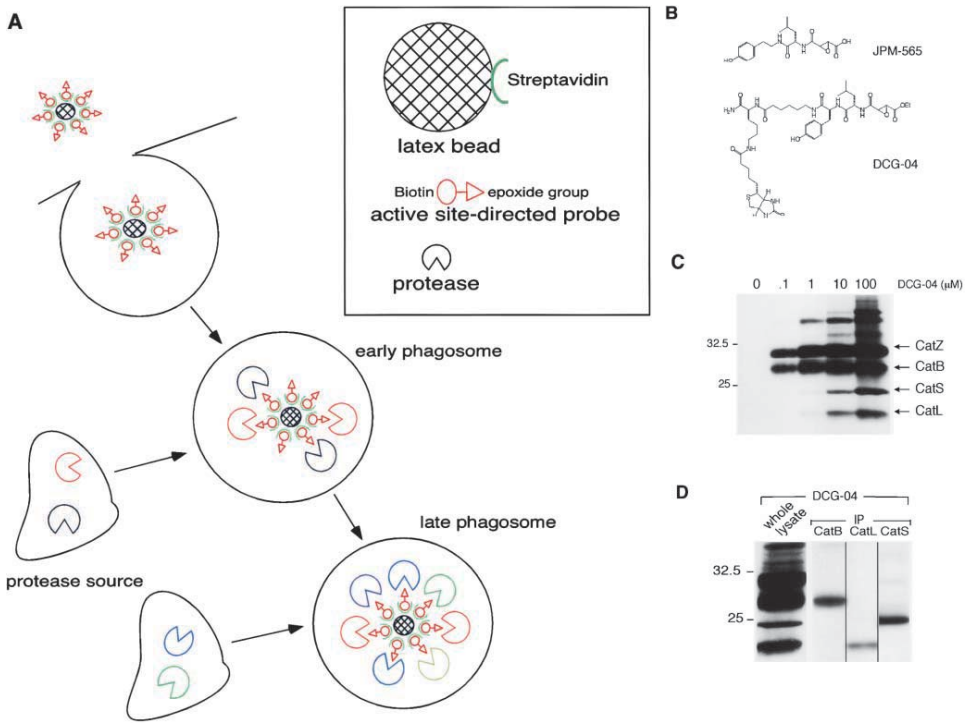

Figure 1. Cysteine proteases recognized by the active site–directed probe DCG-04 in macrophage cell lysates. (A) Schematic overview of the approach designed to examine phagosomal proteolytic contents. To target phagosomal proteases, biotinylated active site–directed probes are coupled to streptavidin-coated latex beads. Upon phagocytosis of the beads, the probe reacts with the active proteases it encounters. Analysis of the modified enzymes at different time points allows a sampling of the proteolytic activities acquired by the phagosome upon fusion with the various endosomal compartments. (B–D) Proteins were separated by SDS-PAGE on a 12.5% gel and reactive proteases were visualized by streptavidin blotting. (B) Structure of the active site–directed probe JPM-565 and its biotinylated derivative DCG-04. (C) Titration of DCG-04 for the labeling of the total cell lysates from J774 cells (pH 5). Lysates were incubated with increasing concentrations of DCG-04. Only the bands in the 15–40-kD range are shown because the larger polypeptides have been shown to be contaminants (reference 18). (D) Identification of individual cysteine proteases labeled by DCG-04. Total extracts from J774 cells (pH 5) were incubated with 5 μM DCG-04 and subjected to immunoprecipitation using anti-CatB, anti-CatL, or anti-CatS antibodies.

suitable for sampling phagosomal proteolytic activities in live phagocytes.

Visualization of Phagosomal Proteolytic Activity In Vivo. To check whether DCG-04–loaded streptavidin-coated beads can be acquired by phagocytes and target cysteine proteases in endosomal compartments, J774 cells were incubated with DCG-04–coated beads according to the procedure outlined in Fig. 2 A. To ensure that an adequate amount of beads was taken up, cells were pulsed with DCG-04–coated beads for 30 min. Excess beads were removed by washing and cells were chased for 60 min to allow the beads to reach the relevant endocytic compartments. At the end of the chase, cells were lysed in reducing SDS sample buffer immediately followed by heating to prevent postlysis modification of proteases by the probe. Samples were resolved by electrophoresis and analyzed by streptavidin blotting to visualize the DCG-04–modified polypeptides. DCG-04 coupled to beads labeled CatZ, CatB, CatS, and CatL, demonstrating that the activity of these four enzymes can indeed be visualized in phagosomes of live cells (Fig. 2 B). By loading the latex beads with increasing concentrations of DCG-04, the signal could be enhanced with maximal labeling being achieved at 0.1 μM DCG-04 (Fig. 2 B).

We performed control experiments to ascertain that the detected proteases were indeed being labeled by the DCG-04 immobilized on the beads. DCG-04 in solution was added to J774 cells to determine if the free compound can be delivered to cysteine proteases by fluid phase endocytosis. We did not detect labeled Cats (Fig. 2 B). To exclude

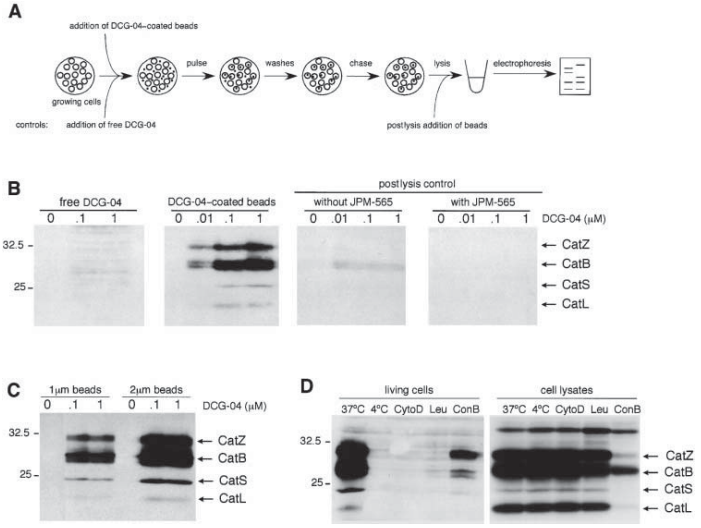

Figure 2. Visualization of phagosomal cysteine protease activity in vivo. (A) Schematic outline of the experimental design. (B–D) Proteins were separated by SDS-PAGE on a 12.5% gel and reactive proteases were visualized by streptavidin blotting. (B) Analysis of phagosomal proteases. J774 cells were incubated for 30 min at 37°C with latex beads previously coated with different concentrations of DCG-04 (pulse). After the removal of excess beads, cells were additionally incubated for 1 h at 37°C (chase). Cells were then directly lysed in 2× concentrated reducing sample buffer. Controls: on the left, cells were treated as in A, but free soluble DCG-04 was added during the pulse instead of DCG-04 coupled to beads, and on the right, cells were treated as in A, but DCG-04–coated beads were added just before lysis in the presence or absence of 100 μM JPM-565. (C) Analysis of phagosomal proteases comparing beads of 1- and 2-μm diameter. J774 cells were incubated for 30 min at 37°C with various concentrations of DCG-04 coupled to latex beads. Cells were then washed in PBS, incubated for an additional 60 min at 37°C, and lysed in sample buffer containing 100 μM JPM-565. (D) Labeling of phagosomal proteases requires phagocytosis. On the left, J774 cells were pretreated with the indicated inhibitors for 60 min (10μg/ml Cytochalasin D, 1mM Leupeptin, or 20 nM ConB), pulsed with beads coupled to 0.1 μM DCG-04 for 30 min at 37°C (lanes 1, 3, 4, and 5) or 4°C (lane 2), washed in PBS, and chased for 60 min at 37°C or 4°C before lysis in reducing sample buffer containing 100 μM JPM-565. On the right, cells were treated as shown on the left except that they were lysed at pH 5. Cell lysates were incubated with 10 μM DCG-04 for 60 min at 37°C. Note that the two differentially glycosylated forms of CatB appear as a doublet at low expression levels (left).

the possibility that proteases liberated upon cell lysis could bind to the probe despite the fully denaturing conditions of the sample buffer, we added DCG-04–loaded beads to cells just before lysis (Fig. 2 B). A very faint band of CatB was detected under these conditions, suggesting that a small fraction of this protease reacts with the probe at the time of lysis (Fig. 2 B). This postlysis labeling could be suppressed when cells were lysed in SDS sample buffer, to which an excess of nonbiotinylated JPM-565 had been added (Fig. 2 B). For subsequent experiments, an excess of JPM-565 was included in the lysis buffer. Finally, a comparison of 1- and 2-μm beads showed that 0.1 μM DCG-04 was saturating for both bead sizes with a stronger signal for 2-μm beads (Fig. 2 C). We concluded that the amount of protease activities detected is proportional to the amount of probe internalized. Therefore, subsequent experiments were performed with 2-μm beads incubated with 0.1–1 μM DCG-04, and cells were lysed in reducing sample buffer containing an excess of JPM-565.

Additional controls exploring pharmacological inhibitors (Cytochalasin D, Concanamycin B [ConB], and leupeptin) or low temperature demonstrated that protease labeling was dependent on phagocytosis of the DCG-04–coated beads. Cells were incubated with DCG-04–coated beads and chased in the presence of inhibitors or at 4°C (Fig. 2 D). Whole cell lysates from each sample were labeled separately with DCG-04 in solution to determine that the inhibitory effect was due to suppression of phagocytosis rather than a mere reduction in cysteine protease activity (Fig. 2 D). In parallel, fluorescent beads were used to verify whether inhibition of phagocytosis had occurred. Phagocytosis was blocked at 4°C in the presence of Cytochalasin D, an inhibitor of actin polymerization (12), as observed by the absence of colocalization of the fluorescent beads with the lysosomal marker Lamp1 under these conditions (unpublished data). No active cysteine proteases were labeled at 4°C or in Cytochalasin D–treated cells (Fig. 2 D), even though their total activity remained unaffected as shown by labeling of whole cell lysates with DCG-04 in solution (Fig. 2 D). As expected, colocalization of fluorescent beads with Lamp1 was strongly reduced in the presence of ConB (unpublished data), an inhibitor of the H^+ proton–pumping ATPase that blocks orderly transport along the endocytic pathway, especially at the early to late endosome transition (25, 26). ConB itself did not affect the activity of cysteine proteases in lysates as measured by labeling with DCG-04 (Fig. 2 D). When cells were incubated with DCG-04–coated beads and chased in the presence of ConB, the activity of CatS and CatL was no longer detected in the phagosome, whereas CatB activity was greatly reduced (Fig. 2 D). In contrast, CatZ activity was only slightly reduced by exposure to ConB (Fig. 2 D). This is in agreement with the previous observation that CatZ is incorporated into the phagosome early during maturation

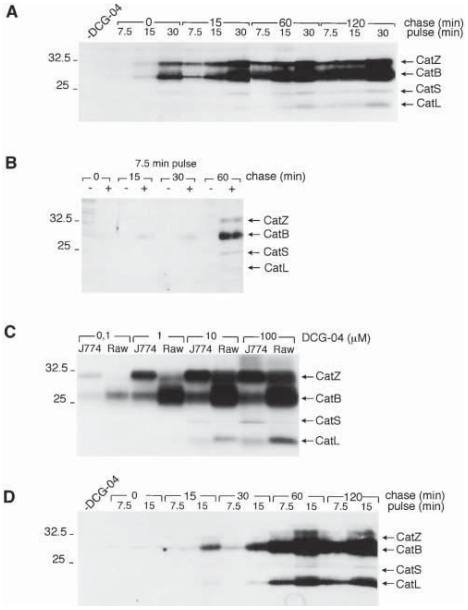

Figure 3. Changes in cysteine protease activity during phagosome biogenesis. (A–D) Proteins were separated by SDS-PAGE on a reducing 12.5% SDS gel and reactive proteins were visualized by streptavidin blotting. (A) Analysis of proteolytic activities incorporated into the phagosome of J774 cells during maturation. Cells were incubated at 37°C with latex beads coupled to DCG-04 as indicated for different periods of time (pulse). After removing excess beads, cells were additionally incubated at 37°C (chase). After each time point, cells were lysed in reducing sample buffer containing 100 μM JPM-565. (B) Purification of phagosomes and analysis of their proteolytic contents. J774 cells were incubated for 7.5 min at 37°C with DCG-04–coated beads (pulse). After removal of excess beads, cells were incubated for the times indicated at 37°C (chase). Subcellular fractionation was then performed using a sucrose gradient. Both phagosomal (+beads) and nonphagosomal fractions (−beads) were recovered and directly lysed in reducing SDS sample buffer. (C) Comparison of the total contents in cysteine proteases of J774 and RAW264.7 (Raw) cells. Lysates (pH 5) were incubated with various concentrations of DCG-04 for 1 h at 37°C. (D) Analysis of proteolytic activities incorporated into the phagosome of RAW264.7 cells during maturation. Cells were treated as in A.

(15) and would therefore be predicted to be resistant to the effect of such H^+-ATPase inhibitors. The protease labeling approach used here indicates that the bulk of CatZ is active in early endosomes, even though the pH in these compartments is only mildly acidic. As expected, although leupeptin, a cell-permeable inhibitor of cysteine proteases (27), had no effect on phagocytosis as assessed by the uptake of beads (unpublished data), it completely abolished DCG-04 labeling in vivo and partially in vitro (Fig. 2 D). We conclude that the labeling of phagosomal proteases by DCG-04–coated beads in living cells is strictly dependent on phagocytosis. Therefore, our approach is suitable to analyze the proteolytic activities to which particles that have been captured by APCs are exposed.

Monitoring Protease Activity During Phagosome Biogenesis. To monitor the activity of individual cysteine proteases at different stages of phagosome maturation, J774 cells were pulsed and chased with DCG-04–coated beads for different times. We observed a time-dependent increase in active protease labeling (Fig. 3 A). As previously shown by Garin et al. (15), this suggests that active cysteine proteases are not delivered into the phagosome synchronously, but rather incorporated gradually. CatZ and CatB activities were the first detected by DCG-04 labeling (Fig. 3 A), which is consistent with the previous observation that both enzymes are present in early endosomes (15). When cells were chased for longer periods, an increase in total labeling was observed, indicating that the more mature phagosomes were also more proteolytically active. Compared with CatZ, the increase in activity of CatB was more substantial at the later time points, consistent with a continuous delivery of active CatB into the maturing phagosome as previously observed (Fig. 3 A; reference 15). We detected active CatS and CatL only after a 15-min pulse and a 30-min chase, with an additional increase at later chase times (Fig. 3 A). After 2 h of chase, CatB, CatS, CatL, and CatZ activities were all established components of phagosomal proteolytic content (Fig. 3 A). No additional increase in signal was observed between 60 and 120 min of chase (Fig. 3 A). This suggests that DCG-04–coated beads may have reached saturation after these longer chase periods (Fig. 3 A), as it was previously shown that CatS is still delivered 12 h after phagosome formation (15).

Do the observed protease activities reflect phagosomal proteolytic content, rather than diffusion of the probe to acidic endosomal compartments? In other words, does DCG-04 remain attached to the beads during endocytic transport? To address these questions, we isolated the bead-containing compartments by a flotation technique (13). Both the compartments that contain DCG-04–coated beads and the remaining membranes were analyzed for protease content by electrophoresis and streptavidin blotting (Fig. 3 B). Although this method allowed us to visualize active proteases targeted by DCG-04, the procedure was less efficient than the more direct phagocytosis assay (Fig. 3 B). Not until 7.5 min of pulse and 60 min of chase was a signal observed (Fig. 3 B), even though sixfold more cells and beads were used than in the experiment shown in Fig. 3 A. Nonetheless, this experiment showed that DCG-04 remains bound to the beads throughout phagolysosomal maturation, because no signal is observed in fractions that lack beads, even though they contain far more protein (Fig. 3 B). We conclude that the protease activities detected by in vivo labeling correspond to active hydrolases incorporated into the phagosome during its maturation.

When we compared lysates prepared from J774 and RAW264.7 cells (a different mouse macrophage cell line) for labeling with increasing amounts of DCG-04, we observed a distinct pattern of labeled proteases. CatB and CatL were more active in RAW264.7 compared with J774 crude cell extracts, whereas there was less CatZ activity

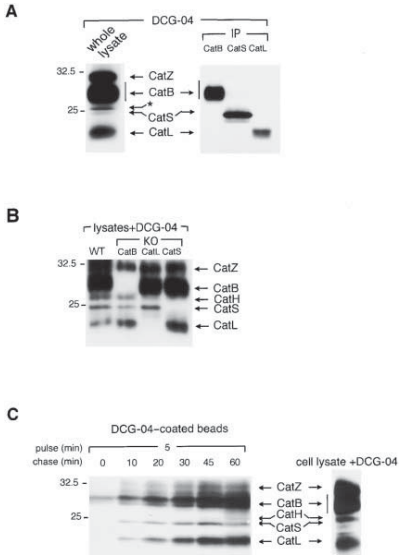

Figure 4. Cysteine protease activity in bone marrow–derived APCs. (A–C) Proteins were separated by SDS-PAGE on a reducing 12.5% SDS gel and reactive proteins were visualized by streptavidin blotting. (A) Analysis of the total contents in cysteine proteases of primary APCs. Total extracts (pH 5) from bone marrow cells cultured in GM-CSF for 6 d were incubated with 0.1 μM DCG-04 for 1 h at 37°C (left). Total extracts (pH 5) were incubated with 5 μM DCG-04 and subjected to immunoprecipitation using anti-CatB, anti-CatS, or anti-CatL antibodies (right). *, a labeled protease of unknown identity specific for bone marrow–derived APCs. (B) Analysis of the total contents in cysteine proteases of primary APCs from WT and Cat-deficient mice. Total extracts (pH 5) from bone marrow cells cultured in GM-CSF for 5 d were incubated with 0.1 μM DCG-04 for 1 h at 37°C. (C) Analysis of proteases incorporated into the phagosome of bone marrow–derived APCs during maturation. Cells cultured in GM-CSF for 6 d were incubated at 37°C with latex beads coupled to DCG-04 for 5 min. After the removal of excess beads, cells were additionally incubated at 37°C (chase). After each time point, cells were lysed in reducing sample buffer containing 100 μM JPM-565.

(Fig. 3 C). Labeling of CatS in RAW264.7 cells was only barely detectable, even at high concentrations of DCG-04 (100 μM), indicating that RAW264.7 has a lower level of active CatS than J774 cells (Fig. 3 C). RAW264.7 cells were then incubated with DCG-04–coated beads and chased for different time periods (Fig. 3 D). As for the J774 cell line, the profile of proteases observed in mature phagosome from RAW264.7 cells is comparable to that seen in total cell extracts labeled with DCG-04 (compare the latest chase points from Fig. 3 A and D with Fig. 3 C). This suggests that in these cells, all endosomal compartments containing cysteine proteases fuse with the phagosome during biogenesis. Our results are therefore consistent with progressive phagosomal maturation in these cell lines, involving distinct endocytic compartments rather than one fusion event with a single target destination, such as the lysosome.

The Phagosome of Primary APCs Selectively Acquires CatS. Do different types of professional APCs use a similar set of endocytic proteases to carry out antigen presentation by class II molecules? Are these proteases accessed in a similar time-dependent manner by internalized particles? How do the distinct APCs modulate the environment of antigens captured by phagocytosis in terms of the proteases they will be exposed to? Having established the methodology for sampling the relevant phagosomal compartments, we applied our protease labeling approach to primary APCs to address these questions.

Mouse bone marrow cells were cultured in GM-CSF, allowing the isolation of two distinct types of professional APCs: DCs ($CD11c^+$) and macrophages ($CD11c^-$; see Fig. 5). The $CD11c^-$ cell population may also contain neutrophils from the granulocyte lineage whose development is equally promoted by GM-CSF. Like macrophages, neutrophils are highly phagocytic cells that are part of the innate immune system but also have the ability to mediate antigen processing and presentation (28). To first analyze the cysteine protease content of bone marrow–derived APCs, day-6 cultures were directly lysed at pH 5 and labeled with soluble DCG-04. Although the activity of CatZ, CatB, CatS, and CatL was detected in these primary APCs, they displayed a more complex pattern of active cysteine proteases than the J774 and RAW264.7 cell lines. In particular, we observed an additional labeled protein migrating at a mass slightly larger than CatS, which was not seen in J774 and RAW264.7 cell lysates (Fig. 4). DCG-04 modification followed by streptavidin-mediated retrieval of the polypeptide and mass spectrometry allowed us to identify it as CatH. The labeling of cells from CatB, CatS, and CatL knockout mice showed that the labeled polypeptides identified as corresponding to these enzymes by immunoprecipitation do not include any other protease (Fig. 4 B). In addition, the presence in bone marrow APC lysates of a labeled polypeptide that comigrates with CatL could be inferred from labeling bone marrow APCs from CatL knockout mice (longer exposed blots; unpublished data). Additional analysis will be needed to establish the identity of this protease.

Next, we performed an in vivo analysis of individual protease activities incorporated into the maturing phagosome of bone marrow–derived APCs. As observed for J774 and RAW264.7 cells, the intensity of the signal increases in a time-dependent manner (Fig. 4 B), demonstrating that active proteases are progressively delivered to the phagosomal compartment. However, the relative amount of active CatZ incorporated into the phagosome was considerably lower than the total amount of active CatZ detected in whole cell lysates (Fig. 4, A and B). This indicates that phagosomes of primary APCs show only limited fusion with compartments containing CatZ compared to what we observed in J774 and RAW264.7 cells. Although the same applies to CatH, the opposite is true for the late endocytic protease CatS. Even though little CatS activity is detected in whole cell lysates (Fig. 4 A), relatively large amounts of active CatS are

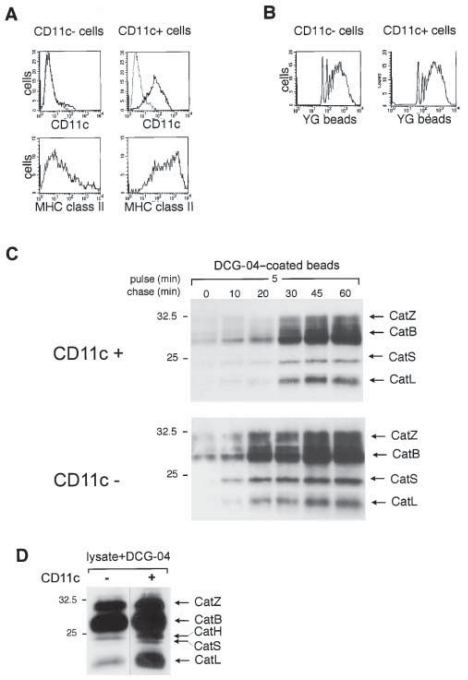

Figure 5. Different rates of protease acquisition by the phagosome of macrophages and DCs. (A) Surface expression of CD11c (top) and MHC class II (bottom) surface in sorted bone marrow–derived APCs. Cells were treated as described in C (see below), incubated with the appropriate antibody, and analyzed by cytofluorometry. Dotted line in top shows isotype control antibody. (B) Uptake of fluorescent latex beads by sorted bone marrow–derived APCs. Cells were treated as described in C. The cells that did not internalize beads (~50%) are not depicted in the histogram because FACS® settings were chosen to visualize the high fluorescence population only. (C–D) Proteins were separated by SDS-PAGE on a 12.5% gel and reactive proteases were visualized by streptavidin blotting. (C) Analysis of proteases incorporated into the phagosome of macrophages ($CD11c^-$) and DCs ($CD11c^+$). Cells cultured in GM-CSF for 6 d were incubated for 5 min at 37°C with fluorescent yellow beads coupled to DCG-04. Excess beads were removed and cells were separated into $CD11c^+$ and $CD11c^-$ cells by MACS at 4°C. Equal cell numbers were additionally incubated at 37°C (chase). After the chase, cells were lysed in reducing sample buffer containing 100 μM JPM-565. (D) Analysis of the total content of cysteine proteases of macrophages ($CD11c^-$) and DCs ($CD11c^+$). Cells were treated as described in C. $CD11c^-$ and $CD11c^+$ cells were lysed at pH 5 and incubated for 60 min with 5 μM DCG-04 at 37°C.

detected in the phagosome (Fig. 4 C). Furthermore, CatS activity is detected earlier during phagosomal biogenesis in primary APCs compared with the macrophage cell lines (compare Fig. 3 and Fig. 4 C). Thus, we conclude that in primary APCs, phagolysosomal fusion preferentially involves endocytic compartments enriched in CatS.

Delivery of Proteases to Phagosomes Is Down Modulated in LPS-activated APCs As mentioned above, mouse bone marrow cells cultured in GM-CSF allow the isolation of two distinct types of professional APCs: DCs ($CD11c^+$, MHC class II^+) and macrophages ($CD11c^-$, MHC class II^-; Fig. 5 A and unpublished data). Expression of MHC class II was induced in the macrophage population by IFNγ (unpublished data).

Do DCs and macrophages display different kinetics of phagolysosomal fusion? To address this question, d6-bone marrow–derived APCs were pulsed with DCG-04–coated beads. After the removal of excess beads by washing, cells were separated by MACS for differential CD11c expression. Separations were performed at 4°C to prevent phagosomal maturation. The $CD11c^-$ and $CD11c^+$ populations of cells were analyzed by FACS® to verify correct cell separation (Fig. 5 A). A comparison of the DC and macrophage samples (Fig. 5 C) showed that phagosomal maturation occurs more rapidly in macrophages compared with DCs, with maximum levels of protease activity already reached after 20 min of chase (Fig. 5 C). In contrast, the maturation of the DC phagosome progresses more slowly because an increase in CatB and CatL activity is still observed after a chase of 45 min (Fig. 5 C). The difference between macrophages and DCs is not attributable to different amounts of beads having been acquired by these two cell populations, as shown by FACS® analysis of the uptake of fluorescent beads (Fig. 5 B). In fact, when equal amounts of bead-containing cells were lysed at pH 5 and labeled with soluble DCG-04, it was observed that $CD11c^+$ cells contain more active cysteine proteases than $CD11c^-$ cells (Fig. 5 D). This observation effectively rules out the possibility that the differences observed in the kinetics of phagolysosomal maturation are due to differences in total protease content. Phagolysosomal fusion therefore appears to be a regulated process that varies according to the type of the phagocyte examined.

A remarkable trait of DCs is the phenotypic and functional change evoked by the exposure to inflammatory stimuli, such as bacterial products, e.g., LPS. Indeed, LPS increased B7.2 and MHC class II expression at the surface of our bone marrow–derived DCs (29 and unpublished data). To explore whether phagosome biogenesis in DCs is also modulated by exposure to LPS, day-6 bone marrow cultures were pulsed with DCG-04–coated beads in the presence or absence of LPS for 5 min. After removing excess beads, $CD11c^+$ cells were isolated and chased at 37°C. The comparison of untreated and LPS-treated cells revealed drastic differences in the rates of phagosome maturation (Fig. 6 A). Indeed, the delivery of active proteases to the phagosome is considerably delayed in DCs pulsed in the presence of LPS because even after 60 and 120 min of chase, beads have not yet reached saturation (Fig. 6 A and unpublished data). This difference between LPS-treated and control cells does not result from reduced bead uptake by the cells pulsed in the presence of LPS (Fig. 6 C), nor from different amounts of active cysteine proteases (Fig. 6 B).

We were also interested in defining whether the LPS-induced delay in phagosomal maturation is a DC-specific

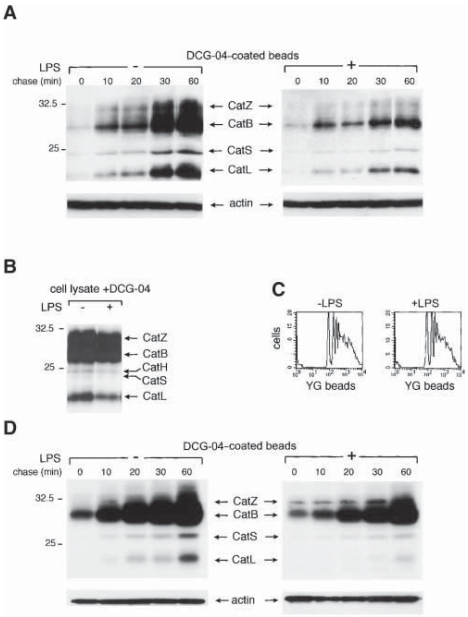

Figure 6. LPS delays phagosome maturation in APCs. (A, B, and D) Labeled proteases were analyzed by SDS-PAGE on 12.5% reducing gel followed by streptavidin blotting. (A) Analysis of proteases incorporated into the phagosome of DCs ($CD11c^+$) upon activation. Bone marrow cells cultured in GM-CSF for 6 d were incubated for 5 min at 37°C with fluorescent yellow beads coupled to DCG-04 in the presence or absence of 0.1 μg/ml LPS. Excess beads were removed and $CD11c^+$ and $CD11c^-$ cells were separated. $CD11c^+$ cells were additionally chased at 37°C. After chase, cells were lysed in reducing sample buffer containing 100 μM JPM-565. (B) Analysis of the total contents in cysteine proteases of DCs treated or not with LPS during a 5-min pulse. Cells were treated as described in A. $CD11c^+$ cells were lysed at pH 5 and incubated for 60 min with 5 μM DCG-04 at 37°C. (C) Uptake of fluorescent latex beads by bone marrow–derived DCs treated or not with LPS during a 5-min pulse. Cells were treated as described in A. The cells that did not internalize beads (~50%) are not depicted in the histogram because FACS® settings were chosen to visualize the high fluorescence population only. (D) Analysis of proteases incorporated into phagosomes of peritoneal macrophages upon LPS activation. Experiments were conducted as described in A.

feature or can be extended to other primary APCs as well. To address this question, we isolated immature peritoneal macrophages and performed uptake experiments with DCG-04–coated beads in the presence or absence o of LPS. In line with the results obtained for DCs, LPS treatment of peritoneal macrophages delayed phagosomal maturation when compared with unstimulated cells (Fig. 6 D). The effect was less dramatic in macrophages than in DCs. After a 60-min chase, the proteolytic content of nontreated and LPS-stimulated macrophages were almost equivalent (Fig. 6 D). We conclude that phagolysosomal fusion, and hence exposure of antigen to the proteases in charge of processing them, is regulated by both the type of APC and the extracellular stimuli they encounter.

Discussion

Here, we describe an approach to directly visualize the activity of proteases that are incorporated into the phagosome at different stages of maturation. Only small numbers of phagocytes are required and there is no need to isolate individual endosomal compartments before analysis. This method is sensitive enough to allow an examination of primary cultures of professional APC, including DCs. Furthermore, the use of covalent active site–directed probes in conjunction with electrophoresis ensures specificity. Methods that employ fluorogenic substrates to detect protease activity suffer from the drawback that more than one enzyme can usually cleave a given peptide substrate. Analysis of the delivery of active hydrolases to the phagosome helped clarify both the distribution of cysteine protease activities among the different endocytic organelles and the dynamics of phagosomal maturation in primary cultures of professional APCs.

We validated our method of in vivo labeling of phagosomal proteolytic activities on the mouse monocytic cell line J774, whose phagosomal protein content has been extensively characterized (15). As shown by others, we found that cysteine proteases are acquired by the maturing phagosome of J774 cells sequentially in a time-dependent manner, and not by delivery together (15). We observed a gradual increase in the phagosomal activity of CatZ, CatB, CatS, and CatL, but the rate of increase was different for the four enzymes examined. We detected CatZ activity early during maturation, which is in agreement with the data of Garin et al. (15) who showed that CatZ is one of the first proteases incorporated into the phagosome. Here, we show that CatZ is not only present but also highly active at this early stage of phagosomal biogenesis even though early endosomes are only mildly acidic, an environment not considered optimal for most lysosomal/endosomal hydrolases. By using a fluorogenic substrate, high levels of CatH activity were observed in the early phagosome (30). However, we did not detect any mature CatH in either J774 phagosomes or crude extracts by our method (unpublished data). Moreover, in the proteomic study performed on J774 phagosomes, CatH was not identified as a phagosomal constituent (15). Because CatH and CatZ show strong sequence homology, we think it is possible that both the fluorogenic substrate and the antibody used to identify CatH activity cross reacted with active CatZ. Although CatS is known to be stable and active at neutral pH in vitro (31), we did detect CatS activity only at later stages of phagosomal maturation. A similar pattern of activity was displayed by CatL, whereas CatB was continuously incorporated into the phagosome. This suggests that active CatL and CatS are present in late endosomal or lysosomal compartments, whereas CatB is active all along the endocytic pathway. These results are in total agree-

ment with the recently published proteasome analysis of the J774 phagosome (13).

We analyzed bone marrow–derived macrophages and DCs by both in vitro and in vivo active site labeling experiments. In vitro labeling of cell lysates with DCG-04 revealed a more complex pattern of proteases in primary APCs compared with the macrophage cell lines analyzed. In both primary macrophages and DCs, we not only detected the activity of CatZ, CatB, CatS, CatH, and CatL, but also that of several additional species of yet unknown identity. By comparing macrophages and DCs, we found that both APC types display an overall similar pattern of active cysteine hydrolases with certain protease activities being higher in DCs. This applied in particular to CatS, which was barely detectable when labeling macrophage cell lysates. In contrast, the levels of CatZ were only slightly increased in DCs.

Application of our in vivo method showed that in contrast to the macrophage cell lines, there is a selective delivery of proteases to the phagosome of primary APCs. In particular, the relative amount of active CatZ incorporated is considerably lower than the amount of active CatZ detected in whole cell lysates. The opposite was observed for CatS. Even though little CatS activity was detected in whole cell lysates, relatively high levels of CatS activity were detected in the phagosome. Labeling intensities for different proteases cannot be directly related to absolute activities, but changes in the ratios of labeling intensities must correspond to shifts in the protease balance. We estimate that the ratio of CatZ to CatS labeling intensity is >10 in cell lysates, whereas it is <1 when examining phagosomes. Phagosomes from primary APCs must therefore fuse preferentially with endocytic compartments enriched in CatS. This finding raises interesting questions about the relevance of CatZ activity for processing of phagocytosed material. A similar observation was made for CatH, whose labeling ratio to CatS is about >10 in cell lysates, whereas it is <1 in the phagosome. Because in J774 cells most CatZ has been found to reside in early endocytic compartments (15 and this study), phagosomes from primary APCs may undergo only limited fusion with early endosomes. However, we cannot exclude that the subcellular distribution of CatZ in primary APCs is different than in J774 cells. Nonetheless, our data show that the incorporation of active proteases into the phagosome of primary APCs is a selective process that ensures delivery of CatS.

We show that phagosomal maturation occurs more rapidly in macrophages than in DCs. Furthermore, we observed a substantial down-regulation of phagosome maturation in DCs exposed to LPS and to a lesser extent, in LPS-treated macrophages. It is possible that this observation results from the ability of such a stimulus to down-regulate endocytosis in DCs. Indeed, a delay in phagolysosomal fusion could result from a more global decrease in the rates of transport along the endocytic axis. The appearance of class II vesicle–like compartments (32) enriched in MHC class II molecules and early endocytic markers has been reported during DC activation (29). This would allow DCs to acquire antigen while minimizing the complete destruction of peptide determinants and therefore be beneficial to ensure T cell activation upon arrival in the lymph node (11). In contrast, macrophages are essential players of the innate immune system, can be microbicidal, and constitute an early barrier against infectious agents. Our measurements of protease activity are consistent with these notions.

Based on the usefulness of active site–directed probes for the analysis of protease activity in live cells, we envision the development of a new generation of compounds that can be coupled directly to antigens of immunological relevance, such as intracellular pathogens, apoptotic cells, or single protein antigens. Analysis of the proteolytic environment to which such materials are exposed upon internalization into the APC should help identify the players involved and the sequence in which they act. Do antigens meet proteases immediately after internalization? Does the proteolytic environment to which antigens are targeted differ for distinct APCs and/or modes of internalization? Do features of the antigen itself or extracellular stimuli affect the proteases to which it is exposed in the APC? Certain pathogens not only inhibit phagolysosomal fusion, but may also encode protease inhibitor homologues that could directly affect the activity of surrounding hydrolases (33). These questions may now be addressed by exploring the proteolytic environment encountered by antigen in the course of trafficking in the APC using methodology similar to that reported here.

The authors thank Christine Kocks, José Villadangos, and Guillaume Duménil for their comments on the manuscript, and Steven Gygi and Larry Lieklider for mass spectrometry analysis.

The authors are recipients of fellowships from the Juvenile Diabetes Foundation (A.M. Lennon-Duménil), Boehringer Ingelheim Fonds (R. Maehr), the Max-Kade Foundation (E. Fiebiger), the Netherlands Organization for Scientific Research (H.S. Overkleeft), and the American Diabetes Association (Cécile Lagaudrière-Gesbert). This work was supported by grants to H.L. Ploegh from the Juvenile Diabetes Foundation International, through the Juvenile Diabetes Research Foundation Center for Islet Transplantation at Harvard Medical School, from the National Institutes of Health (AI34893 and CA14051), from Boehringer Ingelheim, and Fondecyt (project no. 8000011).

Submitted: 27 February 2002
Revised: 28 June 2002
Accepted: 17 July 2002

References

1. Watts, C. 1997. Capture and processing of exogenous antigens for presentation on MHC molecules. *Annu. Rev. Immunol.* 15:821–850.
2. Wolf, P.R., and H.L. Ploegh. 1995. How MHC class II molecules acquire peptide cargo: biosynthesis and trafficking through the endocytic pathway. *Annu. Rev. Cell Dev. Biol.* 11:267–306.
3. Lanzavecchia, A. 1996. Mechanisms of antigen uptake for presentation. *Curr. Opin. Immunol.* 8:348–354.
4. Villadangos, J.A., R.A. Bryant, J. Deussing, C. Driessen, A.M. Lennon-Dumenil, R.J. Riese, W. Roth, P. Saftig, G.P.

Shi, H.A. Chapman, et al. 1999. Proteases involved in MHC class II antigen presentation. *Immunol. Rev.* 172:109–120.
5. Nakagawa, T.Y., and A.Y. Rudensky. 1999. The role of lysosomal proteinases in MHC class II-mediated antigen processing and presentation. *Immunol. Rev.* 172:121–129.
6. Lennon-Dumenil, A.M., A. Bakker, P. Wolf-Bryant, H.L. Ploegh, and C. Lagaudriere-Gesbert. 2002. A closer look at proteolysis and MHC class II-restricted antigen presentation. *Curr. Opin. Immunol.* 14:15–21.
7. Chapman, H.A. 1998. Endosomal proteolysis and MHC class II function. *Curr. Opin. Immunol.* 10:93–102.
8. Watts, C. 2001. Antigen processing in the endocytic compartment. *Curr. Opin. Immunol.* 13:26–31.
9. Arunachalam, B., U.T. Phan, H.J. Geuze, and P. Cresswell. 2000. Enzymatic reduction of disulfide bonds in lysosomes: characterization of a gamma-interferon-inducible lysosomal thiol reductase (GILT). *Proc. Natl. Acad. Sci. USA.* 97:745–750.
10. Maric, M., B. Arunachalam, U.T. Phan, C. Dong, W.S. Garrett, K.S. Cannon, C. Alfonso, L. Karlsson, R.A. Flavell, and P. Cresswell. 2001. Defective antigen processing in GILT-free mice. *Science.* 294:1361–1365.
11. Mellman, I., S.J. Turley, and R.M. Steinman. 1998. Antigen processing for amateurs and professionals. *Trends Cell Biol.* 8:231–237.
12. Ramachandra, L., R. Song, and C.V. Harding. 1999. Phagosomes are fully competent antigen-processing organelles that mediate the formation of peptide:class II MHC complexes. *J. Immunol.* 162:3263–3272.
13. Desjardins, M., N.N. Nzala, R. Corsini, and C. Rondeau. 1997. Maturation of phagosomes is accompanied by changes in their fusion properties and size-selective acquisition of solute materials from endosomes. *J. Cell Sci.* 110:2303–2314.
14. Oh, Y.K., and J.A. Swanson. 1996. Different fates of phagocytosed particles after delivery into macrophage lysosomes. *J. Cell. Biol.* 132:585–593.
15. Garin, J., R. Diez, S. Kieffer, J.F. Dermine, S. Duclos, E. Gagnon, R. Sadoul, C. Rondeau, and M. Desjardins. 2001. The phagosome proteome: insight into phagosome functions. *J. Cell. Biol.* 152:165–180.
16. Lennon-Dumenil, A.M., R.A. Roberts, K. Valentijn, C. Driessen, H.S. Overkleeft, A. Erickson, P.J. Peters, E. Bikoff, H.L. Ploegh, and P. Wolf-Bryant. 2001. The p41 isoform of invariant chain is a chaperone for cathepsin L. *EMBO J.* 20: 4055–4064.
17. Bogyo, M., S. Verhelst, V. Bellingard-Dubouchaud, S. Toba, and D. Greenbaum. 2000. Selective targeting of lysosomal cysteine proteases with radiolabeled electrophilic substrate analogs. *Chem. Biol.* 7:27–38.
18. Greenbaum, D., K.F. Medzihradszky, A. Burlingame, and M. Bogyo. 2000. Epoxide electrophiles as activity-dependent cysteine protease profiling and discovery tools. *Chem. Biol.* 7:569–581.
19. Driessen, C., A.M. Lennon-Dumenil, and H.L. Ploegh. 2001. Individual cathepsins degrade immune complexes internalized by antigen-presenting cells via Fcγ receptors. *Eur. J. Immunol.* 31:1592–1601.
20. Inaba, K., M. Inaba, N. Romani, H. Aya, M. Deguchi, S. Ikehara, S. Muramatsu, and R.M. Steinman. 1992. Generation of large numbers of dendritic cells from mouse bone marrow cultures supplemented with granulocyte/macrophage colony-stimulating factor. *J. Exp. Med.* 176:1693–1702.
21. Shi, G.P., R.A. Bryant, R. Riese, S. Verhelst, C. Driessen, Z. Li, D. Bromme, H.L. Ploegh, and H.A. Chapman. 2000. Role for cathepsin F in invariant chain processing and major histocompatibility complex class II peptide loading by macrophages. *J. Exp. Med.* 191:1177–1186.
22. Meara, J.P., and D.H. Rich. 1996. Mechanistic studies on the inactivation of papain by epoxysuccinyl inhibitors. *J. Med. Chem.* 39:3357–3366.
23. Bryant, P.W., P. Roos, H.L. Ploegh, and A.J. Sant. 1999. Deviant trafficking of I-Ad mutant molecules is reflected in their peptide binding properties. *Eur. J. Immunol.* 29:2729–2739.
24. McIntyre, G.F., and A.H. Erickson. 1991. Procathepsins L and D are membrane-bound in acidic microsomal vesicles. *J. Biol. Chem.* 266:15438–15445.
25. Yilla, M., A. Tan, K. Ito, K. Miwa, and H.L. Ploegh. 1993. Involvement of the vacuolar H(+)-ATPases in the secretory pathway of HepG2 cells. *J. Biol. Chem.* 268:19092–19100.
26. Benaroch, P., M. Yilla, G. Raposo, K. Ito, K. Miwa, H.J. Geuze, and H.L. Ploegh. 1995. How MHC class II molecules reach the endocytic pathway. *EMBO J.* 14:37–49.
27. Amigorena, S., P. Webster, J. Drake, J. Newcomb, P. Cresswell, and I. Mellman. 1995. Invariant chain cleavage and peptide loading in major histocompatibility complex class II vesicles. *J. Exp. Med.* 181:1729–1741.
28. Potter, N.S., and C.V. Harding. 2001. Neutrophils process exogenous bacteria via an alternate class I MHC processing pathway for presentation of peptides to T lymphocytes. *J. Immunol.* 167:2538–2546.
29. Pierre, P., and I. Mellman. 1998. Developmental regulation of invariant chain proteolysis controls MHC class II trafficking in mouse dendritic cells. *Cell.* 93:1135–1145.
30. Claus, V., A. Jahraus, T. Tjelle, T. Berg, H. Kirschke, H. Faulstich, and G. Griffiths. 1998. Lysosomal enzyme trafficking between phagosomes, endosomes, and lysosomes in J774 macrophages. Enrichment of cathepsin H in early endosomes. *J. Biol. Chem.* 273:9842–9851.
31. Riese, R.J., P.R. Wolf, D. Bromme, L.R. Natkin, J.A. Villadangos, H.L. Ploegh, and H.A. Chapman. 1996. Essential role for cathepsin S in MHC class II-associated invariant chain processing and peptide loading. *Immunity.* 4:357–366.
32. Amigorena, S., J.R. Drake, P. Webster, and I. Mellman. 1994. Transient accumulation of new class II MHC molecules in a novel endocytic compartment in B lymphocytes. *Nature.* 369:113–120.
33. Manoury, B., W.F. Gregory, R.M. Maizels, and C. Watts. 2001. Bm-CPI-2, a cystatin homolog secreted by the filarial parasite Brugia malayi, inhibits class II MHC-restricted antigen processing. *Curr. Biol.* 11:447–451.